# Structural configuration of the Teras fault (southern Basin and Range Province) and its rupture in the 3 May 1887 $M_W$ 7.5 Sonora, Mexico earthquake

**Max Suter**

*Instituto de Geología, Universidad Nacional Autónoma de México, Estación Regional del Noroeste, Apartado Postal 1039, 83000 Hermosillo, Sonora, Mexico.*
*SuterMax@aol.com*

**ABSTRACT**

*During the great 3 May 1887 Sonoran earthquake (surface rupture end-to-end length: 101.8 km; $M_W$ = 7.5±0.3), an array of three north-south striking Basin and Range Province faults (from north to south Pitáycachi, Teras, and Otates) snapped along the western margin of the Sierra Madre Occidental plateau. My detailed field survey of the Teras fault and the 1887 earthquake rupture zone along this fault included mapping the rupture scarp and measuring surface deformation at 27 sites.*

*The Teras fault is ~20 km long, strikes N12°E, and has an average dip of 62°W; its maximum throw is >1,640 m and its long-term slip rate >0.08 mm/yr. The fault is structurally simple; it is not internally segmented along strike and does not branch. Striation measurements and the style of faulting indicate extensional dip-slip without significant lateral displacement. In the north, a 2.5-km wide, unbreached right step-over separates the Pitáycachi and Teras faults, whereas the southern limit of the Teras fault is a partly breached relay ramp, where the fault trace shows a 60° bend and jogs to the west. Here, the displacement of the Teras fault is transferred onto the Otates fault and the normal faults bounding the Iglesitas horst.*

*The 1887 surface rupture along the Teras fault (end-to-end length 19.9 km) generally coincides with the mapped trace of the Teras Basin and Range Province fault. Based on 27 measurements, the maximum surface offset is 184 cm and the mean offset 112 cm. The along-rupture surface offset distribution is asymmetric, with the maximum near the southern end of the segment. This suggests that the Teras and Otates segments could be part of a single continuous 1887 rupture that stepped across the structurally complex basement ridge between them. A rough estimate of the average recurrence interval of 1887-size earthquakes on the Teras fault can be obtained from the average slip rate since 23 Ma and the amount of slip on this segment during the 1887 earthquake; the resulting values are 15 to 26 kyr.*

*Key words: southern Basin and Range Province, 1887 Sonoran earthquake, earthquake surface rupture, seismotectonics, earthquake geology.*

**RESUMEN**

*Durante el gran temblor sonorense del 3 de mayo de 1887 (largo de la ruptura: 101.8 km; magnitud $M_W$ = 7.5±0.3), un arreglo de tres fallas con rumbo norte-sur de la Provincia de Cuencas y Sierras —es decir, de norte a sur, las fallas Pitáycachi, Teras y Otates— se reactivaron a lo largo del borde poniente del plateau de la Sierra Madre Occidental. Dentro del estudio de la falla Teras y de la zona de ruptura del temblor de 1887 a lo largo de esta misma falla se cartografió el escarpe de la ruptura y se midieron datos morfológicos-estructurales de la deformación en 27 sitios.*

*La falla Teras tiene ~20 km de largo, un rumbo de N12°E y un echado promedio de 62°; su salto máximo es >1,640 m y su tasa promedio de deslizamiento desde 23 Ma es >0.08 mm/yr. La falla es estructuralmente sencilla; no muestra en planta ni segmentación interna ni bifurcaciones. Este estilo de fallamiento y las estrías medidas indican deslizamiento sobre el plano de falla por extensión, sin componente relevante de desplazamiento lateral. En el norte, un escalón derecho no afallado, de 2.5 km de ancho, separa las fallas Pitáycachi y Teras, mientras que el límite sur de la falla Teras es una rampa de relevo parcialmente rota, donde la traza de la falla muestra un cambio de rumbo de 60° hacia al poniente y su movimiento es transferido tanto a la falla Otates como a las fallas normales que delimitan al horst de Iglesitas.*

*El escarpe de la ruptura sísmica de 1887 a lo largo de la falla Teras mide 19.9 km y coincide en general con la traza geológica de la misma falla. Con base en 27 mediciones, la separación vertical máxima a través del escarpe es 184 cm y el promedio 112 cm. La distribución de estas separaciones a lo largo de la falla es asimétrica, ubicándose el máximo cerca de la terminación sur de la falla. Esto sugiere que los segmentos Teras y Otates pudieran ser partes de una ruptura continua a través del estructuralmente complejo alto de basamento que existe entre los dos segmentos. Una estimación burda del intervalo promedio de recurrencia de temblores de tamaño 1887 se puede obtener a partir de la tasa promedio de deslizamiento de la falla Teras desde 23 Ma y de la cantidad de deslizamiento en el temblor de 1887; los resultados varían entre 15 y 26 kyr.*

*Palabras clave: Provincia de Cuencas y Sierras, temblor sonorense de 1887, ruptura de temblor, sismotectónica, geología de temblores.*

## INTRODUCTION

North-south striking, west-dipping Basin and Range Province normal faults and associated half-grabens form the western edge of the Sierra Madre Occidental plateau in northeastern Sonora, Mexico over a distance greater than 300 km. Slip in 1887 within this segmented normal fault array caused the largest historical earthquake of the southern Basin and Range tectonic-physiographic province and produced the world's longest recorded normal-fault surface rupture in historic time (dePolo *et al.*, 1991; Yeats *et al*., 1997). Field observations indicate that three major range-bounding normal faults ruptured in the 1887 Sonoran earthquake (Suter and Contreras, 2002). The surface rupture dips ~74°W, has a maximum vertical displacement of 5.1 m, and is composed (from north to south) of the Pitáycachi, Teras, and Otates segments (Figure 1). These are the only Basin and Range Province faults in Mexico with known historical earthquake surface rupture. Including two isolated minor segments to the north of the Pitáycachi segment (Figure 1), the 1887 rupture trace adds up to 86.7 km, and the distance between the rupture trace extremities is 101.8 km. Based on the end-to-end length of the rupture trace and the length versus magnitude regression for normal faults by Wells and Coppersmith (1994, tab. 2A), $M_W$ is estimated as 7.5±0.3.

This article focuses on the Teras fault and its rupture in the 1887 earthquake. The first part of the paper documents the stratigraphy and structural configuration of the fault. These regional geologic data are essential to the documentation and interpretation of the new earthquake-related field observations and the understanding of the structural interaction between the Pitáycachi, Teras, and Otates faults. The second part presents in detail the surface rupture of the 1887 earthquake along the Teras fault. Ultimately, these data should be integrated in regional seismic hazard evaluations and will contribute towards a better kinematic model of complex interactions between earthquake rupture segments. Knowledge of the rupture geometry, slip distribution, and fault zone properties is also necessary to understand the spatial distribution of energy dissipation during coseismic slip (Kanamori and Rivera, 2006; Shipton *et al.*, 2006). Moreover, detailed mapping of the rupture geometry is a prerequisite to characterize the rupture propagation, rupture speed, and seismic wave radiation of this earthquake.

The study is based on field mapping, structural and morphological field measurements, and the structural interpretation of digital elevation models and satellite images. The Teras fault is accessible by vehicle on an improved dirt road that leads from Morelos across the Bavispe River to Vega Azul and from there along the 1887 surface rupture past El Toro Ranch, over Puerto El Aire to Pilares de Teras

(Figure 2). Field mapping was based on 1:50,000 scale vertical aerial photographs supplied by *Instituto Nacional de Estadística, Geografía e Informática* (INEGI); these data were subsequently transferred onto the corresponding INEGI 1:50,000 scale topographic map sheets Morelos (H12-B56, 1981) and Colonia Oaxaca (H12-B66, 1982).

## PHYSIOGRAPHY AND VEGETATION

The traces of the Teras fault and the 1887 surface rupture (Figures 1 and 2) are located along the steep western flank of the Sierra Pilares de Teras (in early publications known as Sierra de Teras or Teras Mountains; Aguilera, 1888; Goodfellow, 1888; Bandelier, 1892; Imlay, 1939; White, 1948), at elevations between 860 m and 1,340 m above sea level (asl). Sierra Pilares de Teras is located in a major horseshoe-shaped bend of the Bavispe River (Figure 1). The bend is up to 40 km wide and ~80 km long, and the area within the bend measures ~2,400 km². The name Sierra Pilares de Teras applies to the northern part of the mountain range located within this bend, whereas the southern part of these mountains (and sometimes the entire mountain range within the bend) is known as Sierra El Tigre. No permanent settlements exist within this bend of the Bavispe River with exception of the villages on the river flood plain; the former mining settlements of El Tigre (Figure 1) and Pilares de Teras (Figure 2) are abandoned. The river is at a level of 900 m asl in its eastern part and at 800 m in its western part, whereas the Sierra Pilares de Teras reaches an elevation of ~2,450 m asl. The highest elevations of Sierra Pilares de Teras are located along the Teras fault scarp (Figure 1) due to long-term footwall uplift. The footwall of the Teras fault is characterized by a series of short but deeply incised canyons that are oriented perpendicularly to the fault trace (Figures 1 and 2). Additionally, a narrow fault-controlled valley extends parallel to the fault trace in the hanging wall (Figure 2). These features can be appreciated on a satellite image included in the electronic supplement of a companion paper about the 1887 rupture along the Otates fault (Suter, in press, fig. S2).

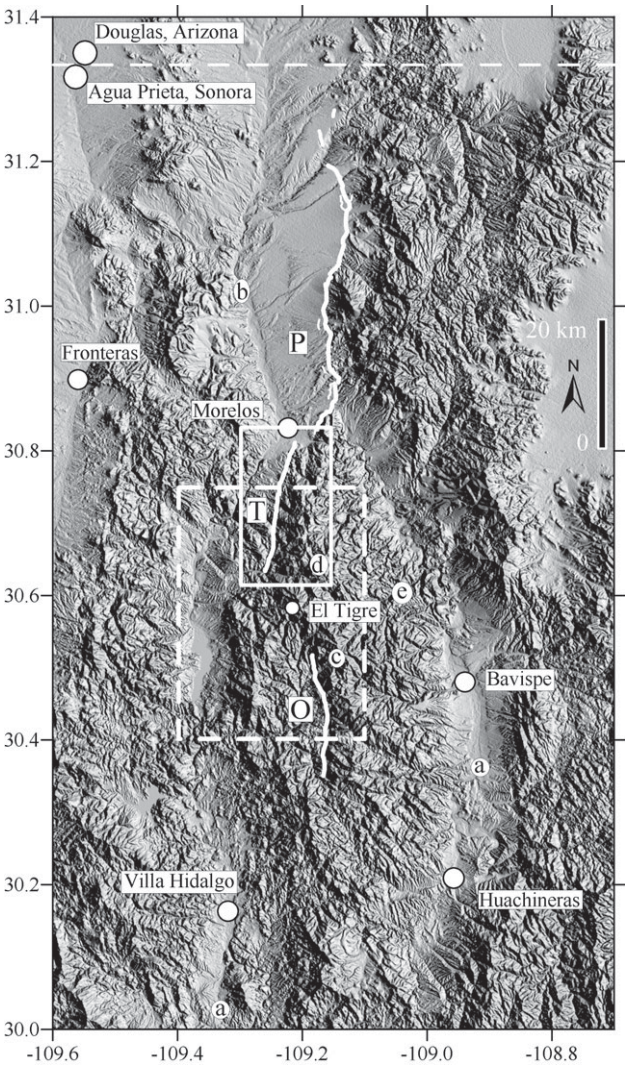


Figure 1. Digital elevation model (Shuttle Radar Topography Mission, 3 arc-second resolution) of northeastern Sonora showing the rupture trace of the 1887 Sonoran earthquake marked by white bold lines (from Suter and Contreras, 2002, modified); P: Pitáycachi segment; T: Teras segment; O: Otates segment; a: Bavispe River; b: San Bernardino River; c: Sierra El Tigre (mountain range within the horseshoe-shaped bend of the Bavispe River); d: Sierra Pilares de Teras (northern part of Sierra El Tigre) and La Carabina canyon; e: La Pita (Santa Rosa) canyon; dashed white line: international boundary. Boxes: regions covered by Figures 2 (solid outline) and 3 (dashed outline).

Due to its location within the horseshoe-shaped bend of the Bavispe River, Sierra El Tigre is a sky-island range within the desert (Felger and Wilson, 1995; Fishbein *et al.*, 1995). The vegetation is conifer forest above 1800 m, oak-grassland between 1800 and 1100 m, and mesquite-grassland and desert scrub below 1100 m (White, 1948; Brown and Lowe, 1994). Differences in vegetation and rates of erosion and sedimentation along the 1887 surface rupture are probably the major reasons for the variable degree of conservation of the rupture scarp. The better-preserved northern (lower) part of the surface rupture is in the desert, whereas the less preserved southern (higher) part, which receives more precipitation, is in grassland and oak forest.

## PREVIOUS STUDIES

Previous studies of the 1887 earthquake focused on intensity distribution and attenuation (DuBois and Smith, 1980; Sbar and DuBois, 1984; Bakun, 2006), regional seismotectonics (Suter and Contreras, 2002), the geomorphology (Bull and Pearthree, 1988; Pearthree *et al.*, 1990) and microseismicity (Natali and Sbar, 1982) of the Pitáycachi segment (Figure 1), and the 1887 surface rupture along the Otates segment (Suter, in press).

The fault along the western margin of the Sierra Pilares de Teras was first reported by Mishler (1920), who indicated between 450 and 920 m of throw. Imlay (1939, p. 1727 and

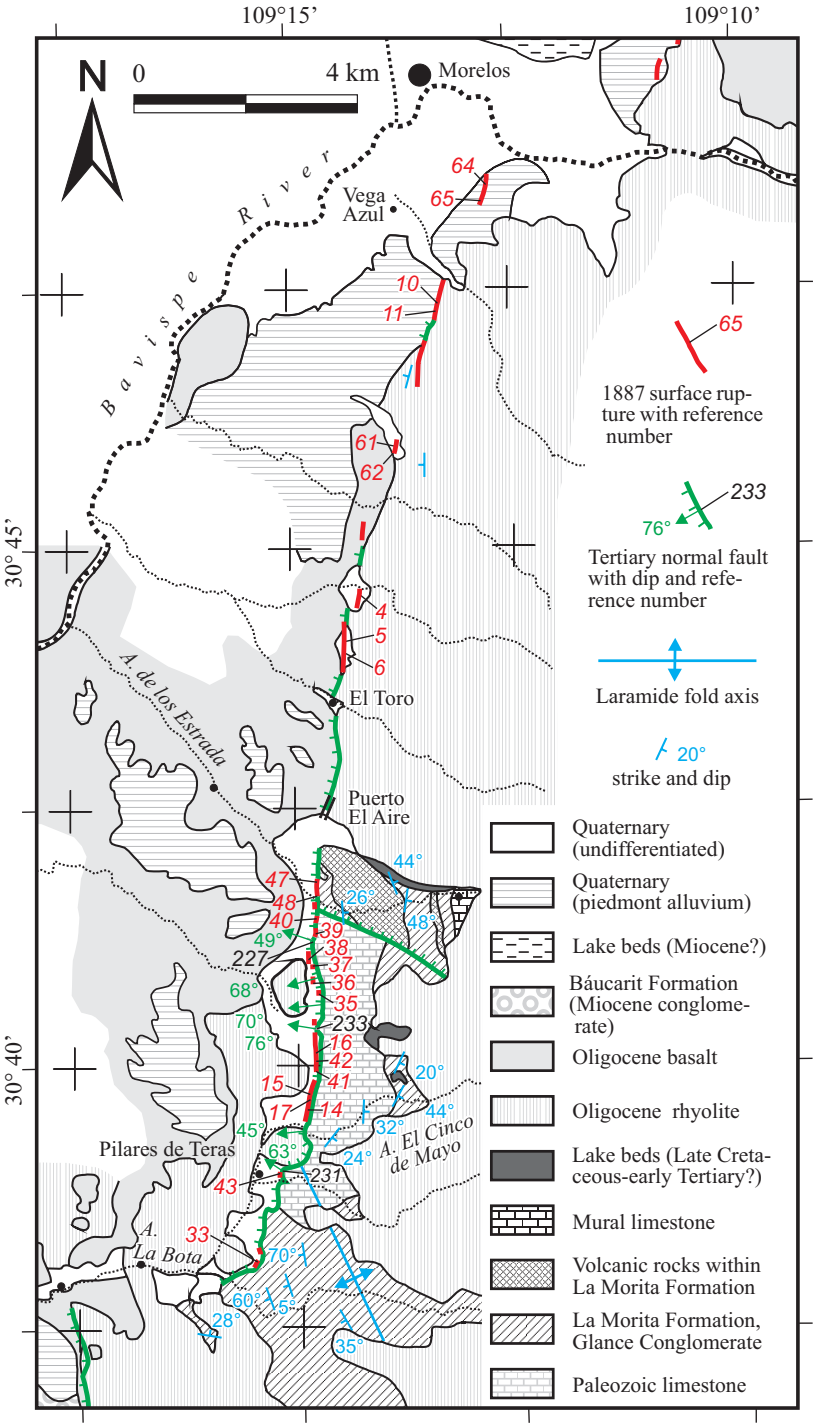


Figure 2. Geologic map showing the measurement sites on the rupture trace of the 1887 earthquake along the Teras fault. Open areas are unmapped.

1732) introduced the name "Teras" for the fault. Both of these authors also mentioned the 1887 surface rupture along the fault but did not provide details, since Mishler's paper was focused on mining and Imlay's work on stratigraphy. Previously, Goodfellow (1888) had mentioned a possible southern continuation of the surface rupture, ~24 km long, beyond the Pitáycachi segment (Figure 1) into the Teras mountain range, based on observations relayed to him by some prospectors. In their unpublished fieldwork in 1980 and 1981, Darrell G. Herd and Catherine R. McMasters of the U. S. Geological Survey traced the surface rupture for 21 km along the Sierra Pilares de Teras following a linear S12°W trend and measured throws of ~1 m (Herd and McMasters, 1982; USGS, 1982, p. 209). The unpublished

rupture trace map by Herd and McMasters was included repeatedly, on a reduced scale, in overview maps of the 1887 rupture (for example, Natali and Sbar, 1982; Nakata *et al*., 1982; Bull and Pearthree, 1988; Wallace *et al.*, 1988; Wallace and Pearthree, 1989; Pearthree *et al.*, 1990; dePolo *et al.*, 1991; Yeats *et al.*, 1997). The trace mapped by Herd and McMasters mostly coincides with the rupture trace documented in this study (Figure 2).

A seismotectonic map of this region including epicenters, focal mechanisms, and the traces of Basin and Range Province faults was provided in Suter and Contreras (2002). A generalized view of the regional geology is given on the INEGI 1:250,000 scale geologic map sheet Nacozari (H12-6, 1983), the 1:500,000 scale geological map of Sonora by Fernández-Aguirre *et al*. (1993), the 1:1,000,000 scale geological map of Sonora by González-León *et al*. (2006), and the *Consejo de Recursos Minerales* 1:50,000 scale geologic map sheet Colonia Oaxaca (H12-B66) by Cerecero-Luna and Castro-Escarrega (1996).

## STRATIGRAPHY

Lithostratigraphic units in the footwall of the Teras fault include Paleozoic limestone, the Cretaceous Bisbee Group, early Tertiary lakebeds, and Early Oligocene felsic volcanic rocks; lithostratigraphic units in the hanging wall of the fault include Early Oligocene felsic volcanic rocks, Oligocene mafic volcanic rocks, Quaternary piedmont alluvium, scree along the fault scarp, and alluvium of the Bavispe River (Figure 2).

About 0.8 km$^2$ of granitic basement (Mishler, 1920; Montaño-Jiménez, 1988) crop out at two locations within the footwall of the Otates fault, 0.5–1.5 km west and southwest of the abandoned mining settlement of El Tigre (Figure 1), where they are faulted against Tertiary felsic volcanic rocks. According to Montaño-Jiménez (1988), this granite is similar in its composition and texture (large pink feldspar megacrysts with Rapakivi texture) to the Precambrian Cananea granite, located ~120 km WNW of El Tigre, which yielded a U-Pb isotope age of 1,440±15 Ma (Anderson and Silver, 1977).

About 5 km$^2$ of Paleozoic marine limestone crop out in the footwall near Pilares de Teras, where they are faulted against Tertiary felsic volcanic rocks and scree (Figure 2). The limestone was studied by Imlay (1939) along Arroyo El Cinco de Mayo (Figure 2), where the section is ~750 m thick and mostly thick-bedded. In this area, the limestone contains diagenetic stylolites, chert, brachiopods, and fusulinids, and is overlain by siliciclastic rocks of the Glance Conglomerate and La Morita Formation (Figure 2). Imlay (1939) correlated the Arroyo El Cinco de Mayo section with the lower part of the section cropping out in La Pita (Santa Rosa) canyon (Figure 1), 15 km farther southeast (Devery, 1979). Paleozoic limestone also crops out (~0.2 km$^2$) in the footwall of the Otates fault (Figure 1), where it is faulted against Tertiary mafic volcanic rocks and talus (Suter, in press, fig. 4). This limestone is coarse to medium bedded, has diagenetic stylolites, and contains recrystallized fusulinids. It is lithologically similar to the Paleozoic marine carbonates reported from La Pita (Santa Rosa) canyon and the Pilares de Teras region.

Previously unmapped outcrops of the Cretaceous Bisbee Group exist along Arroyo de los Estrada (Figure 2). In this section, the Paleozoic limestone is overlain by a 26°E dipping, gray-purplish basal conglomerate (Glance Conglomerate), >50 m thick, with poorly sorted and poorly rounded clasts that are mostly quartzite and partly limestone. The Glance Conglomerate is overlain by ~600 m of felsic lava, with a porphyritic texture, a glassy matrix, ~10% quartz, ~20% feldspars, and no mafics. The lava is overlain by 48°E dipping, well-stratified red mudstone and conglomerate, ~300 m thick; 80% of the components are from the underlying lava, 10% are quartzite, and 10% are limestone. These siliciclastic rocks belong to either the Glance Conglomerate or the La Morita Formation. Up-section follows green-gray felsic lava, ~50 m thick, which may be a Tertiary sill, and which in turn is overlain by more red mudstone and conglomerate of the La Morita Formation, ~150 m thick. These uppermost siliciclastic rocks are overlain by the Aptian-Albian Mural Limestone (Figure 2), which is here composed of oolitic-bioclastic grainstone with chert lenses and 1-m-thick banks of shell hash.

Volcanic rocks interstratified in the Glance Conglomerate and La Morita Formation, similarly to the ones in the Estrada section, have also been observed elsewhere in northeastern Sonora (Cerro La Muella section southeast of Naco; Araujo-Mendieta and Estavillo-González, 1987), northwestern Sonora (Nourse, 2001) and southeastern Arizona (Dickinson and Lawton, 2001, and references therein). The Glance Conglomerate and La Morita Formation in the Estrada section are lithologically similar to the sections described by Montaño-Jiménez (1988) from La Carabina canyon (Figure 1; southernmost east-west drainage on Figure 2) and farther south (his "Conglomerado Carabinas" unit). Large local topographic relief must have existed during the deposition of the Glance Conglomerate and La Morita Formation. In the Estrada section, these rocks are ~1,200 m thick and overlie Permian limestone, whereas 15 km farther southeast, in La Pita canyon, the Glance Conglomerate and La Morita Formation are missing, and the Mural Limestone overlies directly Paleozoic limestone (Imlay, 1939).

On the northern slope of Arroyo de Los Estrada, this Permian-Mesozoic section is overlain with an angular unconformity by horizontally oriented green-yellow greywacke (Figure 2), most likely lake deposits, ~100 m thick, followed up-section by >500 m of Early Oligocene rhyolite of the Sierra Madre Occidental volcanic province (see below). These lakebeds also crop out at two places between Arroyo de Los Estrada and Arroyo El Cinco de Mayo (Figure 2). They are probably of Late Cretaceous

and/or early Tertiary age —younger than the underlying Cretaceous Bisbee Group but older than the overlying Early Oligocene rhyolite— and may belong to the Tarahumara Formation (McDowell *et al*. 2001).

Overlying the Paleozoic limestone and the Cretaceous Bisbee Group with an angular unconformity and locally overlying the Late Cretaceous–early Tertiary lakebeds are ignimbrites, rhyolite, and rhyolitic tuff of the Sierra Madre Occidental volcanic province, which is part of the Cordilleran magmatic-volcanic arc system (Ferrari *et al*., 2005). This volcanic sequence, which is mapped as single unit in this study (Figure 2), is up to ~900 m thick in the Sierra El Tigre and occupies by far the largest part of the footwall of the Teras fault. These rocks are also exposed in the hanging wall along the southern part of the Teras fault. Detailed stratigraphic and petrographic descriptions of these rocks are provided by Mishler (1920) and Montaño-Jiménez (1988) for the region of El Tigre (Figure 1), and by Piguet (1987) and Montigny *et al*. (1987) for the western margin of the Sierra Madre Occidental plateau in the Huásabas – Nacori Chico – Mesa Tres Ríos region, ~100 km farther south. The upper part of this sequence yielded a K-Ar age of 31±1.3 Ma (Early Oligocene) near El Tigre mine (Montaño-Jiménez, 1988). Stratigraphically equivalent ignimbrites of the Boot Heel volcanic field in the southern Peloncillo Mountains, ~70 km north of Sierra Pilares de Teras, yielded $^{40}Ar/^{39}Ar$ ages of 26.8–35.1 Ma (McIntosh and Bryan, 2000).

The Early Oligocene felsic volcanic sequence of the study area is overlain by locally erupted basalt and mafic scoria. In the Nacori Chico – Mesa Tres Ríos region, stratigraphically equivalent basalts have Oligocene K-Ar ages of 26–30 Ma (Montigny *et al.*, 1987; Demant *et al*., 1989). These rocks crop out in the hanging wall of the Teras fault and reach a thickness >500 m where the Bavispe River is carved into them. They are overlain by remnants of Quaternary alluvial fans (Figure 2). Well-indurated, poorly stratified conglomerate and sandstone of the Miocene syntectonic Báucarit Formation crop out in the very southwestern corner of Figure 2; they are part of the fill of the Angostura basin (Figure 3).

Beside alluvial fans, the Quaternary deposits consist of alluvium along the Bavispe River and the arroyos that drain Sierra Pilares de Teras, and scree along the Teras fault south of Puerto El Aire (Figure 2). The scree is typically composed of coarse (0.5–40 cm diameter) unstratified rock debris and covered by desert grassland. In some sections, the lower part of the scree is cemented by carbonate.

## STRUCTURAL CONFIGURATION OF THE TERAS FAULT

The Teras fault delimits Sierra Pilares de Teras on its western side. Similarly to the Otates fault (Suter, in press), the Teras fault is characterized in cross section by a steep footwall escarpment (Figures 1 and 3) that has not retreated with time; no pediment exists either along the Teras or along the Otates fault. The highest elevations of Sierra Pilares de Teras are located along this escarpment due to long-term footwall uplift. The length of the Teras fault is ~20 km and its average strike is N12°E (Figure 2). The average dip of the fault is 62°W based on measurements at six outcrops of the fault plane in Paleozoic limestone (Figure 2). The maximum throw of the Teras fault is >1,640 m as indicated by the offset of the boundary between the felsic and mafic volcanic sequences. This value is based on the elevation of the lowermost outcrops of the mafic sequence in the Bavispe River valley (800 m asl) and the highest elevation of the erosional surface of the felsic sequence in the Sierra Pilares de Teras (2,440 m asl). The footwall is not significantly rotated along the Teras fault; in the Arroyo de los Estrada outcrops (Figure 2), the Late Cretaceous–early Tertiary lakebeds are still horizontal.

In map view the Teras fault is structurally simple; it is not internally segmented along strike and does not branch. The entire fault ruptured in the Sonoran earthquake; the fault trace is practically identical to the 1887 surface rupture (Figure 2). The trace extends from the piedmont alluvium southeast of Morelos in the north to Arroyo La Bota in the south, where the trace shows a 60° bend and jogs to the west. In the north, a 2.5-km-wide right step separates the Teras from the Pitáycachi fault across an unbreached relay ramp (northernmost part of Sierra Pilares de Teras) and the Bavispe River (Figures 1 and 2).

A major transverse basement ridge exists south of the Teras fault (Figure 3). The dogleg at the southern termination of the Teras fault is located at the northern margin of this basement ridge. Structurally, the basement ridge coincides with a fault relay zone where the displacement of the Teras fault is transferred onto the Otates fault and the normal faults bounding the Iglesitas horst. The north-south striking fault separating the Iglesitas horst from the Angostura basin (Figure 3) dips 56° to 78° W; its throw is a minimum of 1,420 m and likely to be ~2,000 m. The fault separating the Iglesitas horst from the Higueras basin (Figure 3) dips subvertically and has a minimum throw of 1,080 m (Suter, in press). There is a 6-km-wide right step in the range-bounding normal fault segments between the Teras fault and the fault delimiting the Iglesitas horst from the Angostura basin (Figures 1 and 3). The step is partly breached by the dogleg of the Teras fault and by a major bend in the trace of the fault delimiting the Iglesitas horst from the Angostura basin (Figure 3).

The region northwest of the basement ridge is a sediment sink characterized by large relict alluvial fans and the valleys of three major arroyos incised into them (Figure 3). The southern two of these arroyos drain the transverse basement ridge, whereas the northern arroyo, La Bota, which has by far the largest catchment area, drains the footwall of the Teras fault (Figure 3). Major sediment accumulation in form of alluvial fans is typical at relay

ramps of en échelon fault arrays (Jackson and Leeder, 1994; Gawthorpe and Leeder, 2000) and has also resulted from numerical experiments of the development of segmented normal fault systems using a model integrating tectonics and surface processes (Contreras and Scholz, 2001).

The hanging walls of the Otates and Pitáycachi faults (Figure 1) are characterized by major alluvial basins. The Higueras basin (hanging wall of the Otates fault; Figure 3) is filled with the syntectonic Báucarit Formation, which consists of as much as 250 m of well-indurated, poorly stratified conglomerate and sandstone (Suter, in press). The basin in the hanging wall of the Pitáycachi fault (Figure 1) is filled with alluvial fan deposits overlying siltstone, thin sandstone, and conglomerate typical of braided stream deposits (Biggs *et al*., 1999), initially described by Aguilera in 1888 (Suter, 2007). Conversely, the Teras fault is a range-front fault with only minor alluviation. The deposits may already have been eroded, since this area is dissected by the Bavispe River (Figures 1 and 3). However, at places where remnants of alluvial fan surfaces are preserved locally (Figure 2), it can be inferred that these fans were <100 m thick. Alternatively, the syntectonic depression formed by the hanging wall of the Teras fault may have been filled by locally erupted basalt and mafic scoria, which cover a large area (Figure 2) and reach a thickness >500 m.

Figure 4 shows an exhumed part of the Teras fault plane in a large natural outcrop at site 227 (Figure 2). The photograph is approximately 15–30 m wide. The 43–56°W dipping fault cuts off Paleozoic limestone and is partly mantled by fault gouge and scree. The fault plane is characterized by major subvertical wear groove striations. Four striations measured at this site and two more from sites 231 and 233 (Figure 2) are shown on a lower hemisphere, equal-area stereoplot (Figure 5). These six striations (Table 1) are a proxy for the 1887 earthquake slip vector, since it is unknown whether they formed during the 1887 event, and since no striations have been observed on the Teras segment of the 1887 surface rupture in surficial deposits. The striations indicate consistently extensional dip-slip motion with a very minor left-lateral strike-slip component. Also

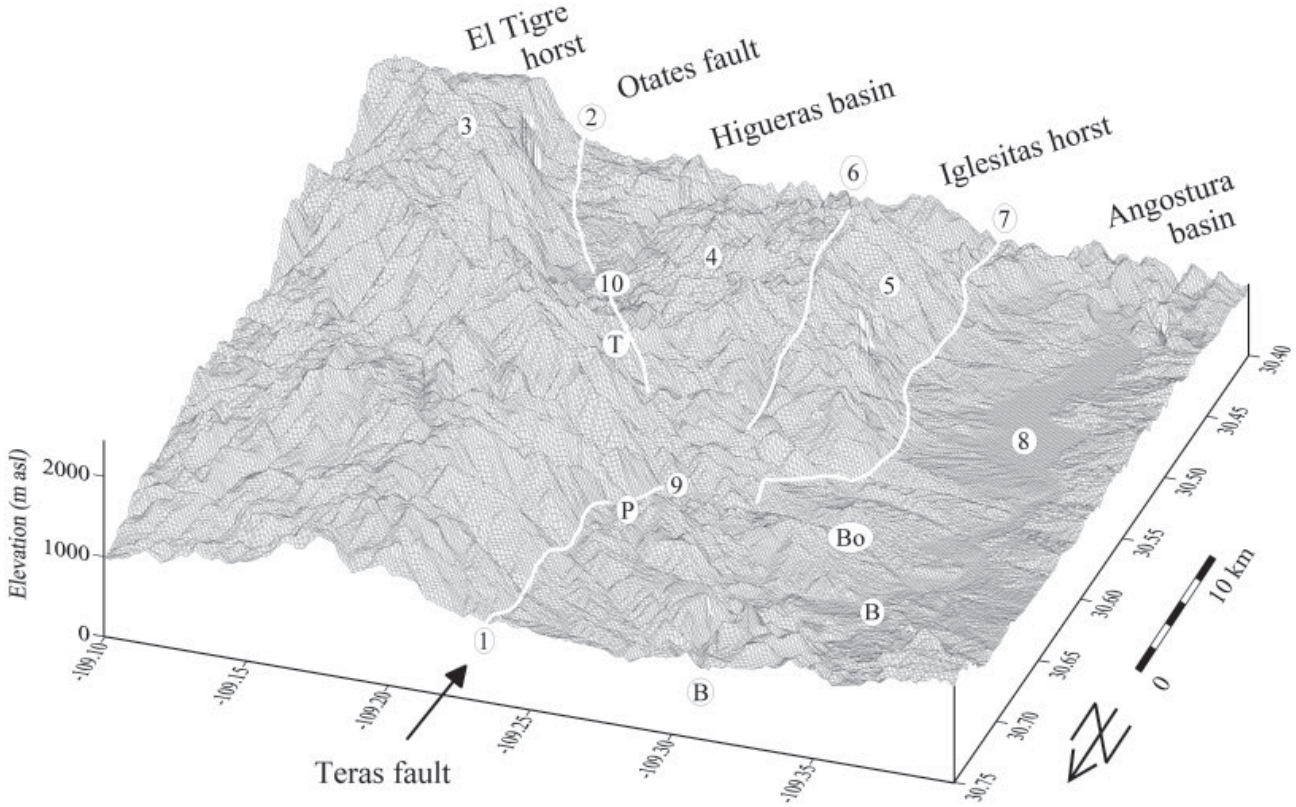


Figure 3. Terrain model showing the fault relay zone where the displacement of the Teras fault is transferred onto Los Otates fault and the normal faults bounding Las Iglesitas horst. The view is from the northwest and 45° from horizontal. The base of the block diagram is at sea level and the maximum elevation at 2,450 m asl. The horizontal distance between neighboring wireframe nodes is 3 arc-seconds (~80 m). The Basin and Range Province structures (approximate traces marked in white) are: 1: Teras fault; 2: Otates fault; 3: footwall of the Otates fault, El Tigre horst (Sierra El Tigre); 4: hanging wall of the Otates fault, Higueras basin, (Los Otates valley); 5: Iglesitas horst (Sierra Las Iglesitas); 6: normal fault delimiting the Iglesitas horst on its eastern side from the Higueras basin; 7: normal fault delimiting the Iglesitas horst on its western side from the Angostura basin; and 8: Angostura basin (now axially drained by the Bavispe River and the Angostura Reservoir). The range-bounding normal fault segments 1 and 7 are separated by a 6-km-wide right step. A major transverse basement ridge (5) is located south of this step. 9 is the southern end of the 1887 surface rupture on the Teras fault, and 10 is the northern end on the Otates fault. T: El Tigre; P: Pilares de Teras; B: Bavispe River; Bo: Arroyo La Bota.

Figure 4. Photograph of the 43–56°W dipping Teras fault plane exhumed on Paleozoic limestone and partly covered by scree at site 227 (Figure 2). The figure is approximately 15–30 m wide. The fault plane is characterized by major vertical wear groove striations that indicate consistently a left-lateral component of motion (Figure 5 and Table 1).

shown on Figure 5 are the P (shortening) and T (extension) kinematic axes corresponding to each measurement, the average P and T kinematic axes (heavy black squares), and the corresponding great circles in form of earthquake focal mechanism nodal planes (T quadrant shaded in grey). They resulted from a kinematic analysis of these fault slip data using the program FaultKinWin developed by Richard W. Allmendinger (version 1.2, 2001, courtesy of ftp://www.geo.cornell.edu/pub/rwa/Windows); see also Marrett and Allmendinger (1990). The fault plane of the focal mechanism strikes N24°E and dips 55°W, whereas the auxiliary plane strikes N1°W and dips 38°E (Figure 5). The result is practically identical to the focal mechanism of the 25 May 1989 M 4.2 earthquake (Wallace and Pearthree, 1989), which had its epicenter ~20 km northwest of the trace of the Teras fault, and is similar to the composite focal mechanism obtained by Natali and Sbar (1982) for well-located microearthquakes near the southern tip of the Pitáycachi segment of the 1887 rupture. The similarity of the focal mechanism presentation of the striations measured on the Teras fault (Figure 5) and the focal mechanism of the 25 May 1989 M 4.2 earthquake (Suter and Contreras, 2002, fig. 2) suggests that this earthquake may have had its source on the Teras fault plane.

From the age of basalt flows intercalated with the lowermost fill of nearby basins (McDowell *et al*., 1997; González-León *et al*., 2000; Paz-Moreno *et al.*, 2003), it can be inferred that the activity of the Teras fault, and Basin and Range Province faulting in the epicentral region of the 1887 earthquake in general, started ~23 Myr ago. The average slip rate of the Teras fault is >0.08 mm/yr based on 23 Myr of fault activity, a maximum throw of 1,640 m, and an average dip of 62°.

## Pre–Basin and Range Province structures within the footwall of the Teras fault

In the Arroyo de los Estrada valley, southeast of Puerto El Aire, the top of the Paleozoic limestone is vertically displaced by 600 m across a NW-SE striking normal fault (Figure 2). The same fault does not displace either the Teras fault or apparently the overlying Oligocene felsic volcanic rocks (Figure 2). Several normal faults of the same orientation were mapped within Sierra El Tigre farther south where they do displace the Oligocene felsic volcanic rocks (Suter, in press; Figure 3).

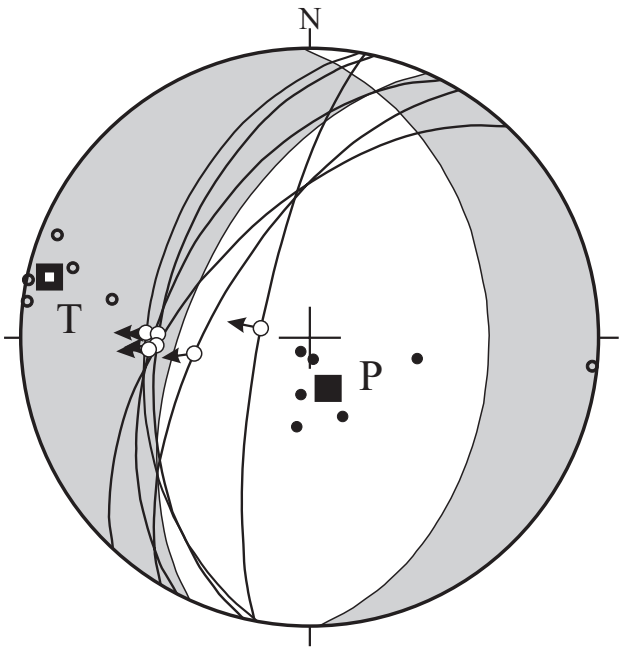


Figure 5. Lower hemisphere, equal-area stereoplot showing the six fault planes and striations measured along the Teras fault (Table 1). P (shortening) and T (extension) kinematic axes are represented by black and open circles, respectively. Average P and T kinematic axes (heavy black squares) and corresponding great circles suggesting earthquake focal mechanism nodal-planes (T quadrant shaded in grey) are also shown. The striations indicate consistently extensional dip-slip motion with a minor left-lateral strike-slip component. The focal mechanism fault plane strikes N24°E and dips 55°W, whereas the auxiliary plane strikes N1°W and dips 38°E.

The Paleozoic limestone and the Cretaceous Bisbee Group within the footwall of the Teras fault dip 20-52°E southeast of Puerto El Aire and in El Cinco de Mayo canyon and up to 70°W in Las Carabinas canyon (Figure 2). The strata in the El Cinco de Mayo – Carabinas region can be interpreted as forming a fold with a NNW-SSE trending axis (Figure 2). Since the lakebeds overlying these rocks southeast of Puerto El Aire are horizontal, it follows that this rotation cannot be due to motion along the Teras fault but is probably entirely the result of Late Cretaceous – early Tertiary Laramide shortening.

## THE 1887 EARTHQUAKE RUPTURE ALONG THE TERAS FAULT

Here I provide a detailed account of the surface rupture of the 1887 earthquake along the Teras fault based on field observations. I mapped the surface rupture as well as the nearby geology at a 1:50,000 scale (Figure 2) and studied the rupture scarp at 27 sites, where I measured the scarp width, scarp height, and the height of the free face (Figure 6, Table 2). At sites with a basal fissure (Table 2), the height and width of the scarp were measured across the fissure. I also noted at each site the material exposed by the fault and, in the case of rock debris, the fragment size, and whether the material is cemented or not. Furthermore, I photographed the 120-year old rupture scarp at several sites (Figures 7 to 10, from north to south).

The 1887 surface rupture along the Teras fault generally coincides with the mapped trace of the fault (Figure 2). The endpoints of the documented surface rupture are located in the south at 109.259°W/ 30.635°N, at an elevation of 1,130 m asl and in the north at 109.212°W/30.810°N at an elevation of 860 m (Figure 2). The length along the rupture trace of the Teras segment is ~20.6 km (Figure 11 and Table 2), whereas the endpoint-to-endpoint distance is 19.9 km. In the northernmost part of the Teras fault, the 1887 surface rupture passes within alluvial fan deposits (sites 64 and 65) or displaces alluvial fans against Tertiary volcanic rocks of the Sierra El Tigre (sites 10 and 11; Figure 2). In the central part of the Teras fault, the rupture passes within Tertiary volcanic rocks in a fault-parallel, long, and narrow valley —erroneously labeled El Tigre valley in Natali and Sbar (1982), Wallace *et al*. (1988), and Wallace and Pearthree (1989)— which passes through El Toro ranch and Puerto el Aire (Figure 2; Suter, in press, fig. S2). Here rhyolite is faulted against basalt, which is partly overlain by relict alluvial fans (Figure 2). Erosion of this tectonically controlled valley and down cutting of the Bavispe River canyon must have occurred after deposition of the alluvial fans. The 1887 rupture was most likely continuous along this part of the fault, but the amount of displacement can only be documented at some few places where the fault-parallel valley is intersected by alluviated east-west valleys draining Sierra El Tigre (Figures 2 and 7). In its southern part (south of Puerto el Aire), the 1887 rupture passes within scree slopes as steep as 22° (Table 2, Figure 9) at the base of the talus formed by the Teras fault, which delimits Permian carbonates and subordinately Mesozoic siliciclastic rocks from Tertiary volcanic rocks (Figure 2). The southern endpoint of the 1887 surface rupture on the Teras fault is north of Arroyo La Bota (Figure 2, site 33), where the fault makes a 60° bend to the west. At several locations, the surface rupture passes only a few meters from the stratigraphic contact between bedrock and scree (Figures 2 and 8-10). Therefore, the earthquake rupture likely coincides with the Teras fault at depth.

Table 1. Fault planes and slip vectors (striations) measured on the surface of the Teras fault in Paleozoic limestone.

| Site | Longitude (°W) | Latitude (°N) | Elevation (m) | Strike (deg) | Dip (deg W) | Rake (deg) | Type of Motion |
|---|---|---|---|---|---|---|---|
| 227 | 109.247 | 30.687 | 1,240 | 27 | 48 | 68 | N-LL |
| | | | | 13 | 47 | 82 | N-LL |
| | | | | 43 | 56 | 60 | N-LL |
| | | | | 10 | 43 | 84 | N-LL |
| 233 | 109.247 | 30.673 | 1,260 | 11 | 76 | 90 | N |
| 231 | 109.253 | 30.650 | 1,180 | 31 | 63 | 70 | N-LL |

The sites are listed from north to south and marked on Figure 2. The vectors are graphed on Figure 6. Horizontal datum: NAD27. N: normal; N-LL: normal–left-lateral

The 1887 surface rupture along the Teras is structurally simple; it is not internally segmented along strike and, unlike the Pitáycachi segment, it has no significant branches or subsidiary faults (Figure 2). An exception is the step faulting observed at site 37 (Table 2), where a minor scarp, with a height of 20 cm, is located 30 m upslope of the main scarp. Small-scale surficial complications could be observed in an exceptionally well-exposed cross section (Figure 8) of the rupture zone directly south of site 35 (Figure 2). The 1887 motion is partitioned there along two west-dipping normal faults, which seem to merge at a shallow depth, and two minor antithetic normal faults. Most of the displacement was along the eastern one of the two west-dipping normal faults, which is in this section partly a shear zone rather than a discrete fault plane. Coarse rock fragments in the lower part of the hanging wall section terminate against this fault, which suggests prior movement along the same fault.

Fault scarp segments steeper than the angle of repose (free faces, Figure 6) still exist at 23 of the 27 observation sites (Table 2). Scarp free-faces are best preserved where the rock debris is cemented. The four sites without a free face (61, 62, 4, and 4A) are located in the recent alluvium of east-west streams draining Sierra El Tigre (Figure 2). The fault scarp slopes range from 12° to 60° (Table 2); the slope is lowest (12° to 19°) at the four sites without free face. The rock debris displaced by the surface rupture is coarse and poorly stratified (Figures 7, 8, and 10) and therefore not suitable for paleoseismological trenching investigation.

**Surface offset and coseismic slip**

The surface offset (vertical separation of the ground surface) was calculated from the scarp height and the slope angle above and below the scarp (Figure 6) (Bucknam and Anderson, 1979; McCalpin, 1996; Yeats *et al*., 1997). The surface offset remains constant, whereas the scarp width and height increase as the scarp broadens with age (Figure 6). Because of the steep, up to 22° inclined slopes adjacent to the 1887 rupture, the surface offset deviates significantly from the scarp height (Table 2). For three of the sites (5, 6, and 36), the calculated surface offset is smaller than the (vertically) measured free face (Table 2) and therefore not useful. This problem did not arise with any of the numerous surface offsets calculated for the Pitáycachi segment but was frequent with the surface offsets computed for the Otates segment (Suter, in press). Because of the steep slopes along the southern part of the Teras fault (Table 2) and especially along the Otates fault, the base of the rupture scarp is often not well defined unless marked by a basal fissure. The transition from the small debris apron at the base of the scarp (Figure 6) to the steep hillslope below is often gradual. Furthermore, the hillslope values used to calculate the surface offset have an uncertainty of ±2°; they were taken from the corresponding INEGI 1:50,000 scale topographic map sheets, which have 20-m contour intervals. The most reliable scarp parameter is the free face (Figure 6), which gives a minimum estimate for the surface offset, whereas the scarp height should give a maximum estimate. For the three sites where the computed surface offset turned out to be smaller than the measured free face (Table 2), I assumed the offset was not more than the free face value (Figure 11). This assumption provides a minimum value for the vertical separation of the ground surface.

A distribution of the surface offsets measured at 27 sites (Table 2) along the rupture trace is shown on Figure 11. The maximum vertical separation is 184 cm at site 15, the minimum vertical separation 51 cm, and the arithmetic average (mean) of the vertical separations is 112 cm. The dashed line on Figure 11 is a linear best fit to the surface offset $y$ values. The regression line corresponds to the function $y = ax + b$, where a = 3.939 and b = 65.15 cm. The correlation coefficient is 0.6020. The along-scarp distribution is asymmetric, with the maximum offset near the southern end of the segment. The high surface offset values at the southern end of the mapped surface rupture of the Teras segment and at the northern end of the mapped surface rupture of the Otates segment suggest that the two segments could be part of a single continuous rupture that stepped across the structurally complex basement ridge between them (Suter, in press). The median of the predicted values (106 cm; y-coordinate for the midpoint of the regression line) is somewhat smaller than the arithmetic average of the individual vertical separation measurements (112 cm).

The ground surface offset distribution can be used to estimate the coseismic slip distribution at depth. The transform from surface offset $y$ to slip $s$ is $s = y / \sin \bar{\alpha}$, where $\bar{\alpha}$ is the average dip of the rupture surface. Since no striations were observed on the surface rupture scarp, the 62° average dip measured on the Teras fault plane (Figure 2) is taken as a proxy. Based on this assumption, the maximum slip along the Teras fault in the 1887 earthquake was 208 cm, the slip resulting from the arithmetic average of the vertical separation measurements was 127 cm, and the slip resulting from the average value of the regression function was 120 cm.

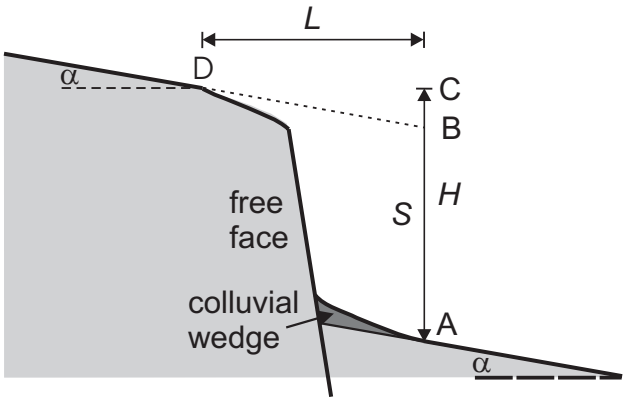


Figure 6. Parameters used to characterize the 1887 surface rupture scarp. The scarp width, scarp height, and the height of the free face were determined with a level and tape measure at 27 sites along the Teras fault (Figure 2 and Table 2). Because of the steep slopes adjacent to the scarp (as much as 22°), the surface offset (*S*) is typically less than the scarp height (*H*).

**Magnitude**

Based on the above slip values and the rupture length, we can estimate the moment magnitude $M_W$ for the rupture of this individual segment from the corresponding empirical scaling laws for normal faults by Wells and Coppersmith (1994). Their maximum displacement-versus-magnitude regression indicates a magnitude of 6.84±0.34 for the 1887 rupture of the Teras fault. Assuming an average displacement of 127 cm, their average displacement-versus-magnitude regression indicates the practically identical magnitude of 6.85±0.33. Based on the 19.9 km endpoint-to-endpoint distance of the rupture trace of the Teras segment, the length-versus-magnitude regression for normal faults by Wells and Coppersmith (1994, tab. 2A) yields a lower $M_W$ of 6.57±0.34 for the 1887 rupture of the Teras fault. These calculations indicate that the aspect (displacement/length) ratio of the 1887 rupture of the Teras fault is somewhat higher than for the average normal fault rupture of the Wells

Table 2. Scarp parameters along the 1887 surface rupture of the Teras fault.

| **Site** | **Longitude** (°W) | **Latitude** (°N) | **Cum. distance** (km) | **Elevation** (m) | **Scarp Height** (cm) | **Scarp width** (cm) | **Scarp slope** (deg) | **Free face** (cm) | **Fissure** (Y/N) | **Surface slope** (deg) | **Surface offset** (cm) |
|---|---|---|---|---|---|---|---|---|---|---|---|
| 64 | 109.213 | 30.808 | 0.20 | 870 | 77 | 120 | 32.7 | 20 | N | 9 | 58 |
| 65 | 109.214 | 30.805 | 0.50 | 880 | 85 | 125 | 34.2 | 40 | N | 11 | 61 |
| 10 | 109.222 | 30.789 | 2.53 | 940 | 130 | 215 | 31.2 | 60 | N | 3 | 119 |
| 11 | 109.222 | 30.788 | 2.68 | 940 | 175 | 268 | 33.1 | 70 | N | 3 | 161 |
| 61 | 109.230 | 30.766 | 5.25 | 980 | 110 | 330 | 18.4 | 0 | N | 9 | 58 |
| 62 | 109.230 | 30.765 | 5.35 | 980 | 100 | 290 | 19.0 | 0 | N | 7 | 64 |
| 4 | 109.237 | 30.743 | 8.07 | 1,000 | 105 | 340 | 17.2 | 0 | N | 6 | 69 |
| 4A | 109.237 | 30.743 | 8.10 | 1,000 | 105 | 515 | 11.5 | 0 | N | 6 | 51 |
| 5 | 109.240 | 30.735 | 9.00 | 1,010 | 115 | 440 | 14.6 | 95 | N | 6 | 29[c] |
| 5A | 109.240 | 30.735 | 9.05 | 1,010 | 165 | 400 | 22.4 | 50 | N | 6 | 87 |
| 6 | 109.240 | 30.733 | 9.25 | 1.020 | 145 | 350 | 22.5 | 110 | Y | 9 | 90[c] |
| 47 | 109.246 | 30.696 | 13.53 | 1,140 | 140 | 190 | 36.4 | 50 | ? | 9 | 110 |
| 48 | 109.246 | 30.694 | 13.80 | 1,140 | 140 | 180 | 37.9 | 80 | ? | 9 | 111 |
| 40 | 109.246 | 30.690 | 14.20 | 1,180 | 160 | 170 | 43.3 | 70 | ? | 10 | 130 |
| 39 | 109.246 | 30.688 | 14.50 | 1,220 | 170 | 220 | 37.7 | 80 | ? | 13 | 119 |
| 38 | 109.248 | 30.684 | 14.95 | 1,230 | 155 | 150 | 45.9 | 70 | ? | 22 | 94 |
| 37 | 109.247 | 30.683 | 15.08 | 1,270 | 140[a] | 120 | 45.0 | 85 | Y | 22 | 92 |
| 36 | 109.247 | 30.680 | 15.40 | 1,250 | 130 | 160 | 39.1 | 100 | ? | 15 | 87[c] |
| 35 | 109.246 | 30.678 | 15.60 | 1,260 | 150 | 200 | 36.9 | 80 | Y | 18 | 85 |
| 16 | 109.247 | 30.669 | 16.68 | 1,270 | 180 | 130 | 54.2 | 145 | Y | 15 | 145 |
| 42 | 109.247 | 30.667 | 16.83 | 1,280 | 185 | 230 | 38.8 | 70 | ? | 11 | 140 |
| 41 | 109.247 | 30.666 | 17.03 | 1,290 | 190 | 160 | 49.9 | 110 | ? | 15 | 147 |
| 15 | 109.248 | 30.662 | 17.45 | 1,230 | 230 | 170 | 53.5 | 120 | Y | 15 | 184 |
| 17 | 109.248 | 30.661 | 17.55 | 1,230 | 210 | 130 | 58.2 | 140 | Y | 13 | 180 |
| 14 | 109.249 | 30.660 | 17.75 | 1,230 | 225 | 130 | 60.0 | 130 | N | 19 | 180 |
| 43 | 109.254 | 30.650 | 18.95 | 1,150 | 160[b] | 140 | 48.8 | 70 | Y | 11 | 133 |
| 33 | 109.258 | 30.636 | 20.60 | 1,140 | 230 | 350 | 33.3 | 120 | N | 15 | 136 |

The measurements (n = 27) are listed from north to south. The sites are marked on Figure 2. Horizontal datum: NAD27. The scarp parameters are defined on Figure 6. [a] Includes the height (20 cm) of a minor scarp, which is located 30 m upslope of the main scarp, and which also has a fissure at its base. [b] The scarp height decreases to nil at the southern tip of this outcrop. [c] At these sites (5, 6, and 36), the computed surface offset is smaller than the (vertically) measured free face (see text for explanations) and therefore not useful. In these cases the free face provides a minimum value for the surface offset.

and Coppersmith (1994) data set. According to their regressions, the typical length of a magnitude $M_W$ 6.85 normal fault rupture is 26.0 km, whereas the maximum and average displacements of a $M_W$ 6.57 normal fault rupture are 160 and 74 cm, respectively.

## Slip rate and recurrence interval

To date, no Quaternary slip rate has been calculated for the Teras fault. Basin and Range Province faults that separate bedrock from internally unfaulted basin fill, such as the Teras fault, typically have vertical slip rates >0.1 mm/yr (dePolo and Anderson, 2000). As mentioned previously, the estimated long-term geologic slip rate of the Teras fault is 0.08 mm/yr based on an estimated throw of 1,640 m along a 62°-dipping fault over a period of 23 Myr. A rough estimate of the average recurrence interval of 1887-size earthquakes on the Teras fault can be obtained from this slip rate and the amount of slip on this segment during the 1887 earthquake; the resulting values are 26 kyr based on the maximum slip, 16 kyr based on the slip resulting from the arithmetic average of the vertical separation measurements, and 15 kyr based on the slip resulting from the average value of the regression function. These estimates are within the range of recurrence intervals documented for normal faults of the southern Basin and Range Province and the Río Grande rift (10 to 100 kyr; Menges and Pearthree, 1989; Machette, 1998).

Conversely, the Quaternary slip rate of the Pitáycachi fault, obtained from the fault scarp morphology and the estimated age of soils formed on alluvial surfaces displaced by the fault, is only 0.015 mm/yr (Bull and Pearthree, 1988; Pearthree *et al*., 1990), twelve times slower than its long-term rate of ~0.18 mm/yr (Suter and Contreras, 2002). Such a decrease of slip rate with time is also characteristic for many faults of the Río Grande rift; the Socorro fault zone, for example, slowed from 0.18–0.20 mm/yr in the latest Miocene, to about 0.05 mm/yr in the Pliocene, and 0.02–0.04 mm/yr in the past 750 kyr (Machette, 1998). Given this

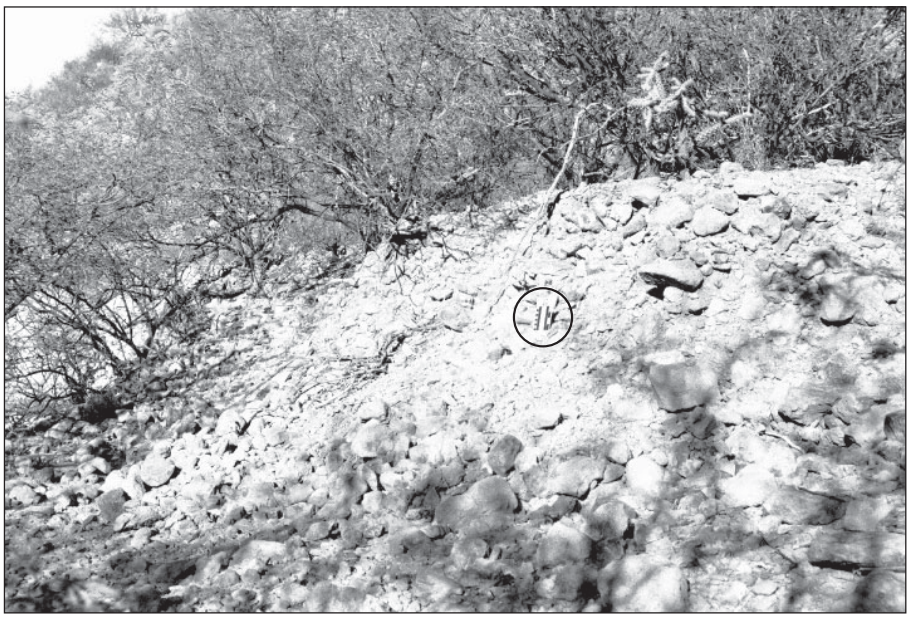

Figure 7. View of the 1887 rupture at site 10 (Figure 2). The height of the scarp measures 119 cm (Table 2). The free face remains in the upper 60 cm of the scarp and exposes uncemented piedmont alluvium of 5–15 cm rock fragment size. A colluvial wedge has developed in the lower part of the scarp. The left part of the circled scale measures 10 cm.

decrease of long-term slip rate with time, the above estimate of the average recurrence interval of 1887-size earthquakes on the Teras fault is likely to be a lower bound.

The change in Coulomb failure stress caused by the rupture of individual segments of a fault zone may advance or delay the rupture of adjacent segments (King *et al*., 1994; Crider and Pollard, 1998; Stein, 1999; Gupta and Scholz, 2000). This suggests that the various segments of the fault zone on the western edge of the Sierra Madre Occidental plateau may have failed in the past in segment combina-

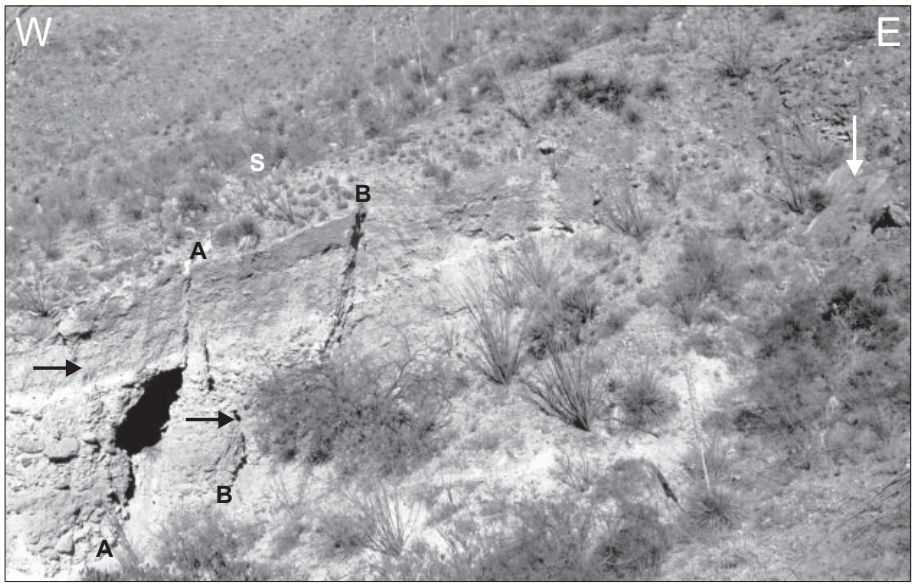


Figure 8. Cross-sectional view of the 1887 surface rupture within scree. The view is from the south. The section is located directly south of site 35 (Figure 2), where the vertical displacement measures 85 cm (Table 2). The surface rupture scarp is marked by the letter S. The Teras fault plane (vertical arrow) can be seen on the very right, ~15 m east of the surface rupture, on Paleozoic limestone. The 1887 motion is partitioned along two west-dipping normal faults, labeled A and B, which seem to merge near the lower margin of this figure, and two minor antithetic normal faults (horizontal arrows). Most of the 1887 displacement was along B, which is partly a shear zone rather than a discrete fault plane. The coarse rock fragments in the lower part of the hanging wall section terminate against B, which suggests prior movement along this fault.

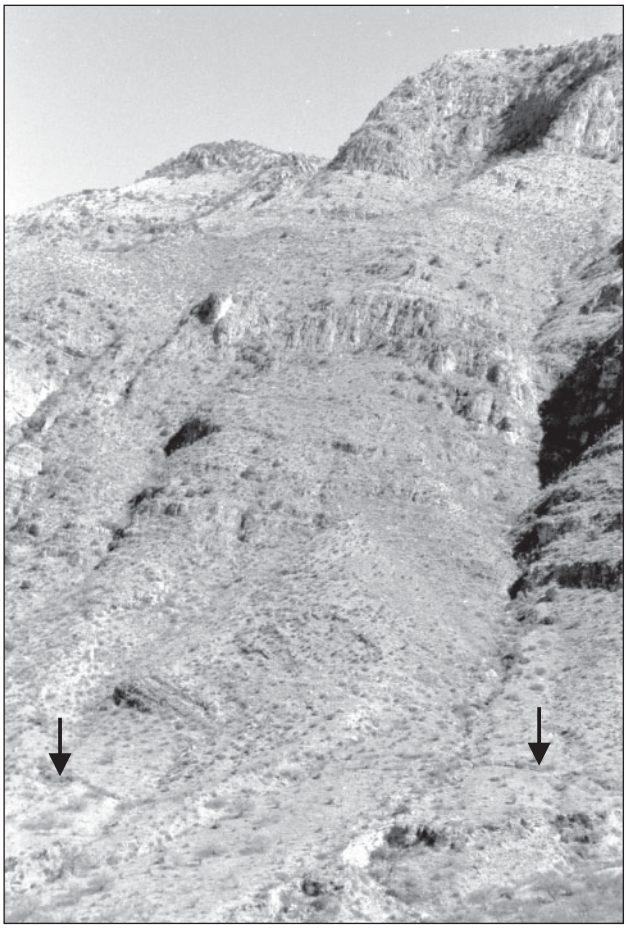

Figure 9. Photograph looking east at the scarp (marked by arrows) of the 1887 earthquake near site 16 (Figures 2 and 10). The rupture trace passes within scree, close to the base of the multi-event Teras fault escarpment, which is composed of Paleozoic limestone. The visible height of the Teras fault scarp is here ~450 m, and the height of the 1887 rupture scarp measures 145 cm (Table 2).

tions that are different from the one that ruptured in 1887 (Pitáycachi-Teras-Otates), which probably results in major fluctuations of the recurrence intervals for the individual fault segments.

## Structural interaction between the Teras and Otates rupture segments

A 15-km-long gap separates the southern end of the Teras segment from the northern end of the Otates segment (Figure 3). Assuming the rupture propagated from north to south, the 1887 rupture was arrested along the southern Teras fault where the fault trace has a 60° bend and jogs to the west. A model of changes in Coulomb failure stress resulting from the 1887 rupture indicates lobes of stress increase at the tips of the rupture segments, especially in the step-over between the Teras and Otates faults (Suter and Contreras, 2002). The northern part of the Otates fault and the northern parts of the normal faults bounding the Iglesitas horst (Figure 3) are located in this zone of stress concentration. Therefore, the 1887 rupture could have either jumped from the Teras to the Otates fault or triggered slip along the faults bounding the Iglesitas horst. However, field-checking the fault traces along the Iglesitas horst did not reveal any obvious morphological or stratigraphic evidence of Quaternary fault activity.

The Teras surface rupture segment has lower surface offset (vertical separation) values than the Otates segment to the south, even though the Teras segment is slightly longer (Suter and Contreras, 2002; Suter, in press). This suggests that the Otates rupture segment may be longer than mapped. This hypothesis is also supported by the high surface offset values at the northern end of the mapped surface rupture of the Otates segment (Suter, in press, fig. 9). Furthermore, the high surface offset values at the southern end of the mapped surface rupture of the Teras segment (Figure 11) and at the northern end of the mapped surface rupture of the Otates segment suggest that the two segments could be part of a single continuous rupture that stepped across the structurally complex basement ridge between them. However, there is no clear evidence of young surface ruptures supporting this hypothesis.

## Structural interaction between the Teras and Pitáycachi rupture segments

Near Morelos, a 2.5-km-wide, unbreached right step-over separates the Pitáycachi and Teras segments of the 1887 earthquake surface rupture across the Bavispe River (Figures 1 and 2). This step-over is also defined by a minimum in the 1887 slip distribution, which suggests that the Pitáycachi and Teras are independent rupture segments that do not merge at depth (Suter and Contreras, 2002). In their approach to the step-over, the traces of the Pitáycachi and Teras rupture segments are characterized on a smaller length scale by right-stepping en échelon patterns (Suter, unpublished data, and Figure 2) indicating a distributed left-lateral component of motion within this transfer zone.

According to observations by Goodfellow (1887), the Pitáycachi and Teras rupture segments overlap. Based on his rupture map (facsimile in Suter, 2006, fig. 3), the Pitáycachi segment continues in the south across the Bavispe River into the Sierra Pilares de Teras for at least 8 km. The same rupture configuration is shown on the map by Aguilera (1888) (facsimile in Suter, 2006, fig. 5). According to Goodfellow (1888), the scarp heights along the Pitáycachi rupture segment in the Sierra Pilares de Teras are ~0.9 m and do not exceed 1.5 m. Both, Goodfellow (1888) and Aguilera (1888) noticed the scarp height attenuation to near zero, approaching either side of the Bavispe River valley, and Goodfellow (1888) observed locally reverse faulting, 3.2 km south of the river. At his southernmost observation point, 8 km south of the river, the scarp height was one

Figure 10. View from the southwest of the 1887 surface rupture displacing scree of the Teras fault at site 16 (Figure 2). The entire scarp profile is formed by free face exposing rock debris composed of coarse, unstratified clasts with a diameter of 2–20 cm. The clasts are cemented by carbonate in the lower part of the profile. The free face is 145 cm high (hammer for scale). A fissure, 1–2 m deep, passes at the base of the scarp. Paleozoic limestone of the Teras footwall can be seen in the background.

foot or less (≤30 cm) and the rupture branched. Since the rupture passes in the Sierra Pilares de Teras within volcanic rocks and is not expressed by a multi-event rupture scarp, I have not been able to confirm Goodfellow's observations. A photograph by C.S. Fly (Suter, 2006, fig. 10) documents the 1887 rupture trace directly south of the river where it separates Tertiary volcanic rocks from scree.

According to independent observations by both Aguilera (1888) and Goodfellow (1888), the aftershocks of the 1887 earthquake were concentrated in the northernmost part of Sierra Pilares de Teras, where the step-over between the Teras and Pitáycachi rupture segments is located. Based on its intensity distribution, the 26 May 1907 Colonia Morelos, Sonora ($I_{max}$ = VIII, $M_l$ = 5.2±0.4) earthquake also seems to have had its origin in this region (Suter, 2001, fig. 4). These earthquakes may have been caused by an increase of static Coulomb stress at the tips of the Pitáycachi and Teras rupture segments (Suter and Contreras, 2002).

### Rupture kinematics

The structural configuration of the 1887 rupture along the Teras fault does not indicate where the rupture originated and how it propagated. Conversely, the surface rupture along the Pitáycachi segment has a well-developed branching pattern (five north-facing bifurcations in the northern part of the segment, two south-facing bifurcations in its southern part), which indicates that the rupture of the Pitáycachi segment initiated in its central part where the polarity of the rupture bifurcations changes (Suter and Contreras, 2002). It is therefore very likely that the rupture first propagated bilaterally along the Pitáycachi fault, from where the southern rupture front jumped across the step-over to the Teras fault and from there to the Otates fault (Figure 1). This scenario is supported by the macroseismic observations made by Aguilera (1888), which indicate that this event was a composite earthquake with the sub-events separated by several seconds. Geological observations indicate that historical Basin and Range Province earthquakes with large magnitudes involved sequential rupture of two or more discrete segments (dePolo *et al.*, 1991; Zhang *et al.*, 1999). Furthermore, in a study of the source parameters of Basin and Range Province earthquakes, Doser and Smith (1989) concluded that earthquakes of magnitude ≥7.0 have complex ruptures best modeled by multiple sub-events. Moreover, the directivity effect of a north-to-south propagating rupture along the southern part of the Pitáycachi fault and the Teras and Otates faults also explains why the isoseismals of this earthquake (Aguilera, 1888; Suter, 2006) are so much elongated in a SSE direction.

## CONCLUSIONS

The Basin and Range Province Teras fault, which forms the steep western flank of Sierra Pilares de Teras in northeastern Sonora, ruptured in the 1887 Sonoran earthquake. Rocks exposed along the Teras fault include Paleozoic marine limestone, a lower part of the Cretaceous Bisbee Group (Glance Conglomerate, La Morita Formation, Mural Limestone), early Tertiary lakebeds, Oligocene

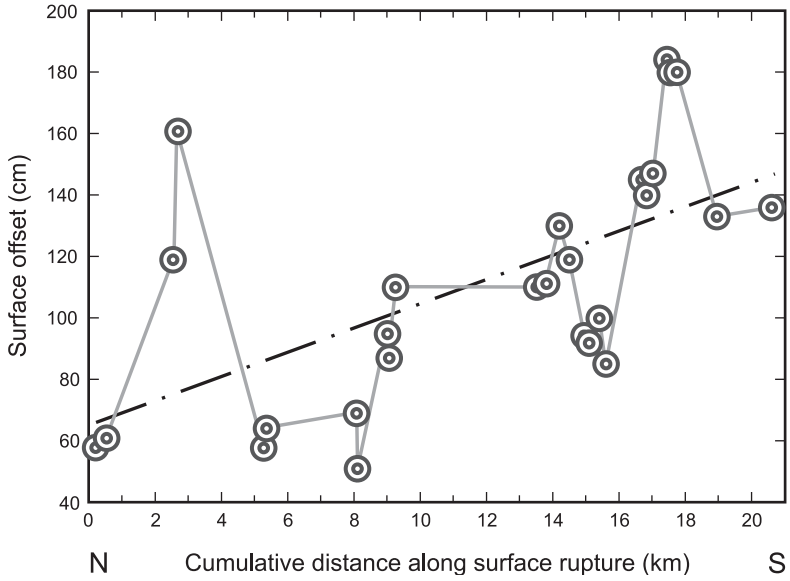


Figure 11. Surface offset measured at 27 locations along the Otates segment of the 1887 earthquake rupture. The maximum vertical offset is 184 cm and the mean offset 112 cm. The dashed line is a linear best fit. The distribution is asymmetric; the maximum surface offset was near the southern end of the rupture. This suggests that the Teras and Otates segments could be part of a single continuous 1887 rupture that stepped across the structurally complex basement ridge between them.

volcanic rocks, and Quaternary piedmont alluvium and scree. In a previously undocumented section along Arroyo de los Estrada, volcanic rocks are interstratified in the Glance Conglomerate and La Morita Formation. A large topographic relief must have existed locally during the deposition of the Glance Conglomerate and La Morita Formation; in the Estrada section, these rocks are ~1,200 m thick and overly Permian limestone, whereas 15 km farther southeast, in La Pita canyon, the Glance Conglomerate and La Morita Formation are missing, and the Mural Limestone overlies directly Paleozoic limestone. The dips measured in the Paleozoic limestone and the Cretaceous Bisbee Group within the footwall of the Teras fault define a NNW-SSE trending fold axis, which must be due to Laramide shortening, since horizontal lakebeds of Late Cretaceous and/or early Tertiary age overly these folded rocks.

The length of the Teras fault is ~20 km, its average strike N12°E, its average dip 62°W, and its maximum throw >1,640 m. At its northern end, a 2.5-km-wide right-step separates the Teras from the Pitáycachi fault across an unbreached relay ramp. In the south, the trace of the Teras fault shows a 60° bend and jogs to the west. A major transverse basement ridge exists south of the Teras fault. The dogleg at the southern termination of the Teras fault is located at the northern margin of this basement ridge. Structurally, the basement ridge coincides with a fault relay zone where the displacement of the Teras fault is transferred onto the Otates fault and the normal faults bounding the Iglesitas horst. There is a 6-km-wide right-step in the range-bounding normal fault segments between the Teras fault and the fault delimiting the Iglesitas horst from the Angostura basin. The step is partly breached by the dogleg of the Teras fault and by a major bend in the trace of the fault delimiting the Iglesitas horst from the Angostura basin.

The 1887 surface rupture along the Teras fault generally coincides with the mapped trace of the fault. The rupture is structurally simple; it is not internally segmented along strike and, unlike the Pitáycachi segment, it has no branches or subsidiary faults. The vertical separation of the ground surface by the rupture scarp (surface offset) was measured at 27 sites; the scarp free face still exists at 23 of these sites. The maximum vertical separation is 184 cm, and the mean of the vertical separations is 112 cm. A linear best fit to the surface offset values shows the along-scarp distribution to be asymmetric, with the maximum offset near the southern end of the segment. The high surface offsets at the southern end of the Teras and at the northern end of the Otates rupture segments suggest that the two segments could be part of a single continuous rupture that stepped across the structurally complex basement ridge between them.

An unbreached right step-over, 2.5-km wide and with an 8-km overlap (Goodfellow, 1887, 1888), separates the northern end of the mapped surface rupture of the Teras segment from the Pitáycachi segment. This step-over is also defined by a minimum in the 1887 slip distribution, which suggests that the Pitáycachi and Teras are independent rupture segments that do not merge at depth. In their approach to the step-over, the traces of the Pitáycachi and Teras rupture segments are characterized on a smaller length scale by right-stepping en échelon patterns indicating a distributed left-lateral component of motion within this transfer zone.

No striations have been observed on the Teras segment of the 1887 surface rupture in surficial deposits. Striations

measured on the Teras fault, which are a proxy for the 1887 earthquake slip vector, indicate consistently extensional dip-slip motion with a very minor left-lateral strike-slip component. The similarity of the focal mechanism presentation of these striations and the focal mechanism of the 25 May 1989 M 4.2 earthquake (Suter and Contreras, 2002, fig. 2) suggests that this earthquake may have had its source on the Teras fault plane.

The surface rupture along the Pitáycachi segment has a well-developed branching pattern (five north-facing bifurcations in the northern part of the segment, two south-facing bifurcations in its southern part), which indicates that the rupture of the Pitáycachi segment initiated in its central part where the polarity of the rupture bifurcations changes. It is therefore very likely that the rupture first propagated bilaterally along the Pitáycachi fault, from where the southern rupture front jumped across the step-over to the Teras fault and from there to the Otates fault.

## ACKNOWLEDGMENTS

I am thankful to Philip A. Pearthree (Arizona Geological Survey) and Craig dePolo (Nevada Bureau of Mines and Geology) for their careful reviews of this manuscript. Financial and logistic support for this work came in part from *Universidad Nacional Autónoma de México* (UNAM) and *Consejo Nacional de Ciencia y Tecnología* (CONACYT, grant G33102-T).

## REFERENCES

Aguilera, J.G., 1888, Estudio de los fenómenos séismicos del 3 de mayo de 1887: Anales del Ministerio de Fomento de la República Mexicana, 10, 5-56.

Anderson, T.H., Silver, L.T., 1977, U-Pb isotope ages of granitic plutons near Cananea, Sonora: Economic Geology, 72, 827-836.

Araujo-Mendieta, J., Estavillo-González, C.F., 1987, Evolución tectónica sedimentaria del Jurásico Superior y Cretácico Inferior en el NE de Sonora, México: Revista del Instituto Mexicano del Petróleo, 19(3), 4-39.

Bakun, W.H., 2006, MMI attenuation and historical earthquakes in the Basin and Range province of western North America: Bulletin of the Seismological Society of America, 96, 2206-2220.

Bandelier, A.F., 1892, Final report of investigations among the Indians of the southwestern United States, carried on mainly in the years 1880 to 1885: Papers of the Archaeological Institute of America, American Series 4, part 2, 591 p.

Biggs, T.H., Leighty, R.S., Skotnicki, S.J., Pearthree, P.A., 1999, Geology and geomorphology of the San Bernardino valley, southeastern Arizona: Arizona Geological Survey, Open-File Report 99-19, 20 p.

Brown, D.E., Lowe, C.H., 1994, Biotic Communities of the Southwest: Salt Lake City, Utah, University of Utah Press, scale 1:1,000,000.

Bucknam, R.C., Anderson, R.E., 1979, Estimation of fault-scarp ages from a scarp-height slope-angle relationship: Geology, 7, 11-14.

Bull, W.B., Pearthree, P.A., 1988, Frequency and size of Quaternary surface rupture of the Pitaycachi fault, northeastern Sonora, Mexico: Bulletin of the Seismological Society of America, 78, 956-978.

Cerecero-Luna, M., Castro-Escarrega, J., 1996, Carta geológico-minera Colonia Oaxaca H12-B66, scale 1:50,000: Secretaría de Comercio y Fomento Industrial, Consejo de Recursos Minerales.

Contreras, J., Scholz, C.H., 2001, Evolution of stratigraphic sequences in multisegmented continental rift basins –Comparison of computer models with the basins of the East African rift system: American Association of Petroleum Geologists Bulletin, 85, 1565-1581.

Crider, J.G., Pollard, D.D., 1998, Fault linkage: three-dimensional mechanical interaction between echelon normal faults: Journal of Geophysical Research, 103, 24,373-24,391.

Demant, A., Cochemé, J.J., Delpretti, P., Piguet, P., 1989, Geology and petrology of the Tertiary volcanics of the northwestern Sierra Madre Occidental, Mexico: Bulletin de la Société Géoloqique de France, Series 8, 5, 737-748.

dePolo, C.,M., Anderson, J.G., 2000, Estimating the slip rates of normal faults in the Great Basin, USA: Basin Research, 12, 227-240.

dePolo, C.M., Clark, D.G., Slemmons, D.B., Ramelli, A.R., 1991, Historical surface faulting in the Basin and Range province, western North America: implications for fault segmentation: Journal of Structural Geology, 13, 123-136.

Devery, J.V., 1979, Sedimentary petrology of the Upper Paleozoic carbonates near Bavispe, Sonora, Mexico: Newark, New Jersey, Rutgers University, M. S. thesis, 79 p.

Dickinson, W.R., Lawton, T.F., 2001, Tectonic setting and sandstone petrofacies of the Bisbee basin (USA–Mexico): Journal of South American Earth Sciences, 14, 475-504.

Doser, D.I., Smith, R.B., 1989, An assessment of source parameters of earthquakes in the Cordillera of the western United States: Bulletin of the Seismological Society of America, 79, 1383-1409.

DuBois, S.M., Smith, A.W., 1980, The 1887 Earthquake in San Bernardino valley, Sonora: State of Arizona, Bureau of Geology and Mineral Technology, Special Paper 3, 112 pp.

Felger, R.S., Wilson, M.F., 1995, Northern Sierra Madre Occidental and its Apachian outliers: a neglected center of biodiversity, *in* Leonard, F., Ffolliott, P.F., Ortega-Rubio, A., Gottfried, G.J., Hamre, R.H., and Edminster, C.B. (eds.), Biodiversity and management of the Madrean archipelago: The sky islands of the southwestern United States and northern Mexico: Fort Collins, Colorado, U.S. Department of Agriculture, Forest Service, General Technical Report RM-GTR-264, p. 36-51.

Fernández-Aguirre, M.A., Monreal-Saavedra, R., Grijalva Haro, A.S., 1993, Carta geológica de Sonora, Hermosillo, Sonora, Mexico, Centro de Estudios Superiores del Estado de Sonora (CESUES), scale 1: 500 000.

Ferrari, L., Valencia-Moreno, M., Bryan, S., 2005, Magmatismo y tectónica en la Sierra Madre Occidental y su relación con la evolución de la margen occidental de Norteamérica: Boletín de la Sociedad Geológica Mexicana, 57, 343-378.

Fishbein, M., Felger, R., Garza, F., 1995, Another jewel in the crown: a report on the flora of the Sierra de los Ajos, Sonora, Mexico, *in* Leonard, F., Ffolliott, P.F., Ortega Rubio, A., Gottfried, G.J., Hamre, R.H., Edminster, C.B. (eds.), Biodiversity and management of the Madrean archipelago: The sky islands of the southwestern United States and northern Mexico: Fort Collins, Colorado, U.S. Department of Agriculture, Forest Service, General Technical Report RM-GTR-264, p. 126-131

Gawthorpe, R.L., Leeder, M.R., 2000, Tectono-sedimentary evolution of active extensional basins: Basin Research, 12, 195-218.

González-León, C.M., McIntosh, W.C., Lozano-Santacruz, R., Valencia-Moreno, M., Amaya-Martínez, R., Rodríguez-Castañeda, J.L., 2000, Cretaceous and Tertiary sedimentary, magmatic, and tectonic evolution of north-central Sonora (Arizpe and Bacanuchi Quadrangles), northwest Mexico: Geological Society of America Bulletin, 112, 600-610.

González-León, C.M., Valencia-Moreno, M.A., Noguez-Alcántara, B., Salvatierra-Domínguez, E., 2006, Mapa geológico de Sonora, México, scale 1:1,000,000: Digital Geosciences, http://digital-geosciences.unam.mx/toc.htm#Gonzalez_2006.

Goodfellow, G.E., 1887, The Sonora earthquake: Science, 10 (236), 81-82.

Goodfellow, G.E., 1888, The Sonora earthquake: Science, 11 (270),

162-166.
Gupta, A., Scholz, C.H., 2000, A model of normal fault interaction based on observations and theory: Journal of Structural Geology, 22, 865-879.
Herd, D.G., McMasters, C.R., 1982, Surface faulting in the Sonora, Mexico, earthquake of 1887 (abstract): Geological Society of America, Abstracts with Programs, 14, p. 172.
Imlay, R.W., 1939, Paleogeographic studies in northeastern Sonora: Geological Society of America Bulletin, 50, 1723-1744.
Jackson, J., Leeder, M., 1994, Drainage systems and the development of normal faults: an example from Pleasant Valley, Nevada: Journal of Structural Geology, 16, 1041-1059.
Kanamori, H., Rivera, L., 2006, Energy partitioning during an earthquake, *in* Abercrombie, R., McGarr, A., DiToro, G., Kanamori, H. (eds.), Earthquakes: Radiated energy and the physics of faulting: American Geophysical Union, Geophysical Monograph Series 170, 3-13.
King, G.C.P., Stein, R.S., Lin, J., 1994, Static stress changes and the triggering of earthquakes: Bulletin of the Seismological Society of America, 84, 935-953.
Machette, M.N., 1998, Contrasts between short-term and long-term records of seismicity, *in* Lund, W.R. (ed.), The Río Grande rift – important implications for seismic-hazard assessments in areas of slow extension, Basin and Range province seismic-hazards summit: Utah Geological Survey, Miscellaneous Publication 98-2, 84-95.
Marrett, R., Allmendinger, R.W., 1990, Kinematic analysis of fault-slip data: Journal of Structural Geology, 12, 973-986.
McCalpin, J.P., 1996, Paleoseismology: San Diego, California, Academic Press, 583 p.
McDowell, F.W., Roldán-Quintana, J., Amaya-Martínez, R., 1997, Interrelationship of sedimentary and volcanic deposits associated with Tertiary extension in Sonora, Mexico: Geological Society of America Bulletin, 109, 1349-1360.
McDowell, F.W., Roldán-Quintana, J., Connelly, J.N., 2001, Duration of Late Cretaceous–early Tertiary magmatism in east-central Sonora, Mexico: Geological Society of America Bulletin, 113, 521-531.
McIntosh, W.C., Bryan, C., 2000, Chronology and geochemistry of the Boot Heel volcanic field, New Mexico, *in* Lawton, T.F., McMillan, N.J., McLemore, V.T. (eds.), Southwest passage, a trip through the Phanerozoic: New Mexico Geological Society Guidebook, Fifty-first Annual Field Conference, 157-174.
Menges, C.M., Pearthree, P.A., 1989, Late Cenozoic tectonism in Arizona and its impact on regional landscape evolution: Arizona Geological Society Digest, 17, 649-680.
Mishler, R.T., 1920, Geology of the El Tigre district, Mexico: Mining and Scientific Press, 121, 583-591.
Montaño-Jiménez, T.R., 1988, Geología del área de El Tigre, noreste de Sonora: Hermosillo, Sonora, Universidad de Sonora, B. Sc. thesis, 135 p.
Montigny, R., Demant, A., Delpretti, P., Piguet, P., Cochemé, J.J., 1987, Chronologie K/Ar des séquences volcaniques tertiaires du nord de la Sierra Madre Occidental (Mexique): Comptes Rendus de l'Académie des Sciences, série II, 304(16), 987-992.
Nakata, J.K., Wentworth, C.M., Machette, M., 1982, Quaternary fault map of the Basin and Range and Rio Grande rift provinces, western United States: U. S. Geological Survey Open-File Report 82-579.
Natali, S.G., Sbar, M.L., 1982, Seismicity in the epicentral region of the 1887 northeastern Sonora earthquake, Mexico: Bulletin of the Seismological Society of America, 72, 181-196.
Nourse, J.A., 2001, Tectonic insights from an Upper Jurassic–Lower Cretaceous stretched-clast conglomerate, Caborca–Altar region, Sonora, Mexico: Journal of South American Earth Sciences, 14, 453-474.
Paz-Moreno, F.A., Demant, A., Cochemé, J.J., Dostal, J., Montigny, R., 2003, The Quaternary Moctezuma volcanic field: A tholeiitic to alkali basaltic episode in the central Sonoran Basin and Range province, México, *in* Johnson, S.E., Paterson, S.R., Fletcher, J.M., Girty, G.H., Kimbrough, D.L., Martín-Barajas, A. (eds.), Tectonic evolution of northwestern México and the southwestern USA: Geological Society of America, Special Paper 374, 439–455.
Pearthree, P.A., Bull, W.B., Wallace, T.C., 1990, Geomorphology and Quaternary geology of the Pitaycachi fault, northeastern Sonora, Mexico, *in* Gehrels, G.E., Spencer, J.E. (eds.), Geologic excursions through the Sonoran desert region, Arizona and Sonora: Arizona Geological Survey, Special Paper 7, 124-135.
Piguet, P., 1987, Contribution à l'étude de la Sierra Madre Occidental (Mexique): La séquence volcanique tertiaire de la transversale Moctezuma – La Norteña: Université de Droit, d'Economie et des Sciences d'Aix-Marseille, Faculté des Sciences et Techniques de St-Jérome, Thèse pour obtenir le grade de Docteur en Sciences, 208 p.
Sbar, M.L., DuBois, S.M., 1984, Attenuation of intensity for the 1887 northern Sonora, Mexico earthquake: Bulletin of the Seismological Society of America, 74, 2613-2628.
Shipton, Z.K., Evans, J.P., Abercrombie, R.E., Brodsky, E.E., 2006, The missing sinks: Slip localization in faults, damage zones, and the seismic energy budget, *in* Abercrombie, R., McGarr, A., DiToro, G., Kanamori, H. (eds.), Earthquakes: Radiated energy and the physics of faulting: American Geophysical Union, Geophysical Monograph Series 170, 217-222.
Stein, R.S., 1999, The role of stress transfer in earthquake occurrence: Nature, 402, 605-609.
Suter, M., 2001, The historical seismicity of northeastern Sonora and northwestern Chihuahua, Mexico (28-32° N, 106-111° W): Journal of South American Earth Sciences, 14, 521-532.
Suter, M., 2006, Contemporary studies of the 3 May 1887 $M_w$ 7.5 Sonora, Mexico (Basin and Range Province) earthquake: Seismological Research Letters, 77, 134-147.
Suter, M., 2007, The first geologic map of Sonora: Boletín de la Sociedad Geológica Mexicana, 59, 1-7.
Suter, M., in press, Structural configuration of the Otates fault (southern Basin and Range Province) and its rupture in the 3 May 1887 $M_W$ 7.5 Sonora, Mexico earthquake: Bulletin of the Seismological Society of America.
Suter, M., Contreras, J., 2002, Active tectonics of northeastern Sonora, Mexico (southern Basin and Range Province) and the 3 May 1887 $M_W$ = 7.4 earthquake: Bulletin of the Seismological Society of America, 92, 581-589.
United States Geological Survey (USGS), 1982, Geological Survey Research 1982 (Fiscal Year 1981): U.S. Geological Survey, Professional Paper 1375, 424 p.
Wallace, T.C., Pearthree, P.A., 1989, Recent earthquakes in northern Sonora: Arizona Geology, 19 (3), 6-7.
Wallace, T.C., Domitrovic, A.M., Pearthree, P.A., 1988, Southern Arizona earthquake update: Arizona Geology, 18 (4), 6-7.
Wells, D.L., Coppersmith, K.J., 1994, New empirical relationships among magnitude, rupture length, rupture width, rupture area, and surface displacement: Bulletin of the Seismological Society of America, 84, 974-1002.
White, S.S., 1948, The vegetation and flora of the region of the Río de Bavispe in northeastern Sonora, Mexico: Lloydia, 11(4), 229-302.
Yeats, R.S., Sieh, K., Allen, C.R., 1997, The geology of earthquakes: New York, Oxford University Press, 568 p.
Zhang, P., Mao, F., Slemmons, D.B., 1999, Rupture terminations and size of segment boundaries from historical earthquake ruptures in the Basin and Range Province: Tectonophysics, 308, 37-52.

Manuscript received: June 17, 2007
Corrected manuscript received: December 10, 2007
Manuscript accepted: December 12, 2007